Computer modelling of the plasma chemistry and plasma-based growth mechanisms for nanostructured materials

Annemie Bogaerts, Maxie Eckert, Ming Mao, Erik Neyts

Computer modeling of the plasma chemistry and plasma-based growth mechanisms for nanostructured materials

Annemie Bogaerts, Maxie Eckert, Ming Mao and Erik Neyts
Research group PLASMANT, Department of Chemistry, University of Antwerp,
Universiteitsplein 1, B-2610 Wilrijk-Antwerp, Belgium
E-mail: Annemie.bogaerts@ua.ac.be

Abstract

In this review paper, an overview is given of different modeling efforts for plasmas used for the formation and growth of nanostructured materials. This includes both the plasma chemistry, providing information on the precursors for nanostructure formation, as well as the growth processes itself. We limit ourselves to carbon (and silicon) nanostructures. Examples of the plasma modeling comprise nanoparticle formation in silane and hydrocarbon plasmas, as well as the plasma chemistry giving rise to carbon nanostructure formation, such as (ultra)nanocrystalline diamond ((U)NCD) and carbon nanotubes (CNTs). The second part of the paper deals with the simulation of the (plasma-based) growth mechanisms of the same carbon nanostructures, i.e., (U)NCD and CNTs, both by mechanistic modeling and detailed atomistic simulations.

1. Introduction

Low temperature plasmas are playing an increasingly important role for the formation and growth of nanostructures and nanostructured materials (e.g., [1-7]). To improve the performance of these plasma growth processes, a good insight is desired in the plasma and in the interaction with the growing nanostructures. This insight can be obtained by experimental research, but the latter is not always straightforward, in view of the small dimensions of the nanomaterials and the possible disturbance of the plasma characteristics, e.g., when introducing a probe. Therefore, computer simulations can be very useful to assist in the experimental developments.

In the present paper, we will give an overview of different modeling efforts that have been presented in the literature for plasmas used for nanostructure formation. This includes two different aspects. First, a thorough understanding of the plasma behavior is needed. This comprises background gas flow and heating (i.e., fluid dynamics), gas breakdown, transport and heating of the electrons and the so-called heavy particles, as well as the plasma chemistry, i.e., creation and destruction of the various plasma species by chemical reactions. Modeling of the plasma chemistry can give indications on which species are important precursors for the growth of nanostructured materials and how the plasma operating conditions can be tuned to optimize the growth process. Therefore, in this paper we will mainly focus on the plasma chemistry modeling. Several plasma modeling approaches exist in literature, such as analytical models, zero-dimensional (0D) chemical kinetics simulations, fluid models (describing the chemical kinetics as well as fluid dynamics), solving the Boltzmann transport equation, Monte Carlo (MC) and particle-in-cell (PIC)-MC simulations, as well as hybrid methods, combining the above (e.g., MC + fluid) models. For describing the plasma chemistry, the 0D chemical kinetics approach is often applied, as it can take into account a large number of different species and reactions without too much computational effort. However, it assumes a spatially uniform plasma composition and does not consider transport of the plasma species throughout the reactor. The latter is accounted for in the fluid approach, which is based on solving the first three moments of the Boltzmann transport equation, i.e., conservation of mass, momentum and energy. This approach still has a reasonable calculation time, and is therefore also very suitable for describing the plasma chemistry. However, at very

low gas pressure, it is more accurate to describe the electron behavior with a microscopic non-equilibrium model, such as MC simulations, while the other plasma species are treated with the fluid approach, giving rise to hybrid MC-fluid models. In this paper, some examples will be presented on these three different modeling approaches for describing the plasma chemistry for nanoscience applications.

The second aspect involves the interaction of the plasma with the growing nanostructures. This can be simulated by phenomenological, mechanistic models or by detailed atomistic descriptions of the nucleation and growth process. For the nanostructure growth modeling, input from the plasma simulations, such as the fluxes of species arriving at the substrate, is desirable. Vice versa, the plasma-surface interactions provide boundary conditions for the plasma simulations, such as sticking coefficients and surface reaction probabilities at the walls.

In our research group, we are active in the two above-mentioned fields. Therefore, the literature overview will be complemented with some examples from our own research. Although several different types of nanostructured materials can be produced in plasmas [1], we will focus here only on silicon and (especially) carbon nanostructures, more specifically (ultra)nanocrystalline diamond ((U)NCD) and carbon nanotubes (CNTs).

2. Plasma modeling for nanoscience applications

2.1. Modeling of nanoparticle formation in plasmas

The formation of nanostructures and nanostructured materials by means of plasma can be accomplished within the plasma or at a substrate. In the first case, plasma ions or radicals chemically react with each other to form larger plasma species (so-called nucleation or critical cluster formation). The nuclei or clusters will further grow into nanoparticles by coagulation. Eventually, micrometer sized particles can be formed, which will finally be pulled out of the plasma reactor due to gravity.

The study of nanoparticle formation in plasmas is important from several points of view. Initially the nanoparticles were solely considered harmful, because they can contaminate a growing film. In the microelectronics industry, particles can be deposited on the wafer and cause voids, delamination and interconnect shortcuts, thereby “killing” the semiconductor devices [8,9]. Later on, however, it has been shown that nanoparticles can also be beneficial for certain materials science applications [1,8]. For instance, in the case of solar cell production, it has been demonstrated that Si nanoparticles can be incorporated in an amorphous film, giving rise to the formation of so-called polymorphous Si films, which seem to have improved properties for solar cell applications, in terms of stability against light induced defect creation [8,10]. Furthermore, silane-based plasmas have also been used for the gas phase synthesis of silicon quantum dots [11]. More in general, there is a growing interest in plasma-grown nanoparticles as they are considered as the fundamental building blocks of nanotechnology [1].

Several research groups have presented computer modeling for studying the nanoparticle formation mechanisms and the behavior of these particles in plasmas, in order to assist in the experimental research for either minimizing/avoiding undesirable particles in the microelectronics industry or optimizing particle formation for improved film properties. Modeling can be particularly useful for studying the initial formation and growth mechanisms, because this stage is experimentally the most difficult to investigate due to the small particle sizes (few nm), requiring sophisticated diagnostics [12]. For silane plasmas, Boufendi and Bouchoule stated that particles are indeed formed due to successive reactions in the gas phase, i.e., so-called plasma polymerization, whereas the surface did not play a significant role [13,14]. Furthermore, it was demonstrated already in the early 90s by several authors [15-17] that negative ions are the most important particle precursors, as they are

trapped in the bulk plasma and therefore have a longer residence time. Gallagher presented a 0D plasma chemistry model to calculate the evolution of SiH_3^- anions and SiH_m radicals into $Si_xH_m^-$ and Si_xH_m, which further grow into silicon hydride particles [18,19]. A similar 0D chemical kinetics model, in which linear and cyclic silicon hydride species up to 10 Si-atoms were considered, was developed by Bhandarkar et al. [20].

De Bleecker et al. have applied a 1D fluid model to describe the detailed plasma chemistry, and to identify the main precursors, for critical cluster formation in silane plasmas [21,22]. The model incorporates silicon hydrides (Si_nH_m) containing up to 12 Si atoms. In total, 68 species, including molecules, radicals, ions and electrons, and more than 100 chemical reactions, were taken into account in the model. It was confirmed that anion-induced chain reactions are the main pathway leading to nanoparticle formation.

Besides modeling the nucleation stage, also the charging and transport of larger particles needs to be investigated to control the particle behavior. Indeed, nanoparticles immersed in a plasma will become charged by collecting plasma ions and electrons. As the electron mobility by far exceeds the ion mobilities, the particles typically acquire a negative equilibrium charge, the magnitude of which strongly depends on the particle size and plasma conditions. Furthermore, the nanoparticles are subject to several different forces in the plasma, including the electrostatic force, the neutral drag force and ion drag force (resulting from collisions with neutral gas molecules and ions, respectively, causing momentum transfer from the molecules/ions to the nanoparticles), the thermophoretic force (induced by a temperature gradient in the plasma), and the gravity force. The latter is only important for micrometer-sized particles, and can be neglected for nanoparticles, compared to the other forces. Several authors have focused on the charging [23-25] and transport [26,27] of particles in undisturbed plasmas, i.e., without self-consistently including the effect of the nanoparticles on the plasma behavior. The latter has been accounted for by Akdim and Goedheer [28]. De Bleecker et al. have further extended that model, by coupling the nucleation mechanisms with the charging and transport of nanoparticles of predefined sizes [29,30]. The charging is described by the orbital motion limited (OML) theory, yielding an average charge of the particles. The stochastic fluctuations superimposed on the equilibrium charge were not yet taken into account. The importance of the different forces (i.e., electrostatic and ion drag force) was investigated in [29]. The neutral drag force was included as a damping force on the nanoparticle velocities, as no gas flow was considered in the model. It was demonstrated that the density profiles of nanoparticles of different sizes are strongly affected by the relative importance of the different forces. For particles less than 30 nm in size, the electrostatic force is predominant, yielding a density profile with a maximum in the center of the discharge. Larger particles will mainly experience the ion drag force, and are pushed towards the reactor boundaries until the ion drag force is balanced by the electrostatic force. This leads to the trapping of the nanoparticles near the sheath-bulk interface [29]. In [30] the influence of the thermophoretic force, due to a thermal gradient in the plasma induced by heating or cooling one of the electrodes, was investigated. A significant shift of the particle density profiles towards the cooler electrode was observed, even for a temperature difference of about 20-40 K [30]. Recently, a very similar model, including the same chemical kinetics as in [21,22] and considering also charging and transport, was presented by Liu et al. [31] for a dual-frequency capacitively coupled silane discharge. The authors showed that the nanoparticle density and charge distribution were mainly influenced by the voltage and frequency of the high-frequency source; however, the voltage of the low-frequency source can accelerate the nanoparticle formation [31].

In [29-31] nanoparticles of predefined sizes were considered and the exact growth mechanism by coagulation was not yet taken into account. Growth by coagulation was described with a simple chemical reaction scheme for a silane plasma in [32], assuming a

uniform electron density and energy, and neglecting charging of particles. Another simple model for silicon particle coagulation based on Brownian motion was presented in [33], again assuming constant positive ion and electron densities.

Kortshagen and Bhandarkar solved the so-called general dynamic equation, adopted from aerosol physics, in a 0D model, to obtain the particle size distribution by coagulation [34]. The latter approach, but in 1D, was also adopted by De Bleecker et al. [35]. Furthermore, the coagulation model was fully coupled with the initial stage of particle formation by nucleation, and also the charging of the particles and the effect of the various forces discussed above, were accounted for. A flowchart of the coupling between these various parts of the model is illustrated in figure 1. The number density and charge distribution profiles were presented for particles ranging in size from ~0.8 to 50 nm [35].

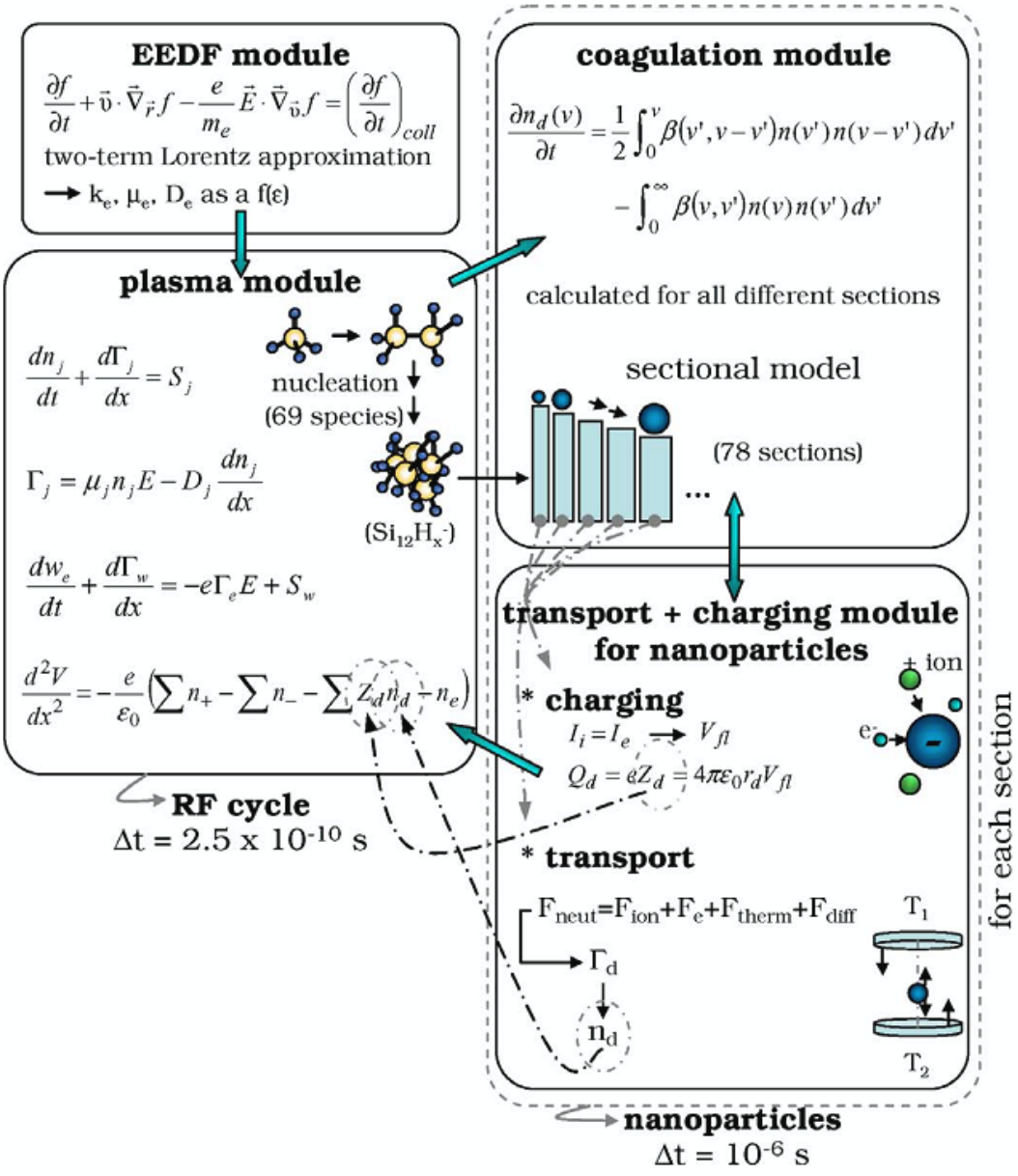

<u>Figure 1:</u> Flowchart of the coupling between different models applied to describe nanoparticles in silane plasmas, including the growth based on nucleation and coagulation, as well as the charging and transport under the influence of different forces.

The latter models, however, neglected the effect of particle charges on the coagulation rate. This effect was investigated for an Ar plasma by Schweigert and Schweigert [36]. Lee and Matsukas showed that particle charge fluctuations can increase the coagulation rate, especially for smaller particles [37]. Lemons et al. developed an analytical model for coagulation between large negatively charged particles and smaller neutral particles [38]. Kim and Kim presented a more detailed numerical model for coagulation between large and small particles, each group having a certain charge distribution [39, 40]. They used a sectional model for the particle size distribution, with size-dependent coagulation coefficients, including the effect of Coulomb forces for coagulation between oppositely charged particles. Warthesen and Girshik developed a detailed model for the spatiotemporal evolution of the nanoparticles, treating both the plasma and aerosol behavior self-consistently, although neglecting the detailed plasma chemistry [41]. This model was further improved by Ravi and Girshik [42], assuming that particle nucleation does not only occur in a rapid burst, but continues to be important in regions free of nanoparticles. Moreover, the effect of an image potential induced by the neutral particles was taken into account. It was found that coagulation is dominated by the collision between small (~1-2 nm) neutral particles and larger negatively charged particles trapped in the plasma. Furthermore, coagulation ceases when the spreading of the nanoparticle cloud across the plasma quenches gas-phase nucleation [42].

Apart from silane discharges, nanoparticle formation also occurs in hydrocarbon plasmas (mainly in acetylene) [43,44]. Some modeling efforts were presented in literature to study the initial stage of nanoparticle formation in acetylene discharges. Stoykov et al. developed a 0D chemical kinetics model that describes the growth of linear chain and cyclic hydrocarbon molecules up to 10 C atoms [45]. A 1D fluid model, containing 41 different species (up to 12 C atoms) and 92 different reactions was presented by De Bleecker et al. [46]. Both positive and negative ion reaction pathways were found to result in a fast build up of the carbon skeleton, although the negative ion pathway will probably be dominant because of the trapping of negative ions in the plasma [46]. In [47] this model was further extended to 55 species and 140 reactions, by including also polycyclic aromatic hydrocarbons. Because the calculated densities of these species were fairly high, it was suggested that aromatic compounds might play a role as growth precursors for nanoparticles in hydrocarbon plasmas [47]. Another improvement of this model was presented by Ming et al. [48]. Indeed, based on a comparison with experimental data, some new mechanisms for negative ion formation and growth, arising from dissociative electron attachment of (linear and branched) hydrocarbons ($C_{2n}H_2$), were proposed. In total, the model now contains 78 different species and about 400 chemical reactions. In general, reasonable agreement with experiment is obtained, although further refinements would still be possible, indicating that in reality the plasma chemistry leading to nanoparticle formation in hydrocarbon (and silane) plasmas is even more complicated.

2.2. Modeling the plasma chemistry for the growth of nanostructured materials

(a) NCD and UNCD:

Nanostructured materials can also be grown directly on a substrate, i.e., the nucleation then takes place at the solid phase rather than in the plasma. Polycrystalline diamond films, among which ultrananocrystalline and nanocrystalline diamond (UNCD and NCD, respectively), produced by plasma deposition, have very promising tribological, biological and electrical applications [49-51]. NCD films are typically grown under conventional diamond PE-CVD conditions, i.e., a CH_4/H_2 mixture at a ratio 1/99, and a substrate temperature above 1000 K [52], resulting in columnar diamond crystals with diameters below 500 nm [51]. UNCD films, on the other hand, embody ball-like diamond grains with sizes of typically a few nm [51], and can be grown in a hydrogen-poor plasma ($CH_4/Ar/H_2$ in a ratio

of 1/97/2) at a substrate temperature as low as 700 K [52]. A scheme of the PE-CVD process of nanostructured diamond can be found in figure 2.

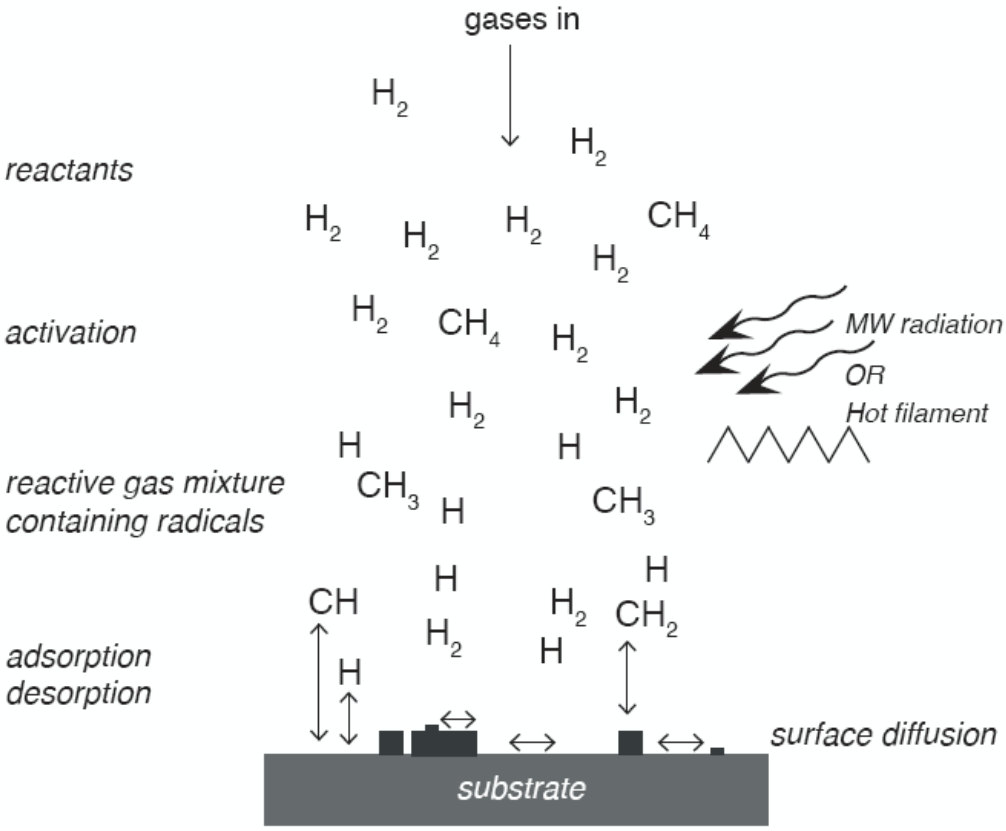

Figure 2: Schematic description of the PE-CVD process for (U)NCD, based on an illustration in Ref. [53]. (U)NCD can be deposited by hot filament CVD or microwave PE-CVD (MW PE-CVD). (U)NCD films grown by means of MW PE-CVD are nowadays the technique of choice. The activation of the gas mixture does not contaminate the growing film, as it is an electrode-free discharge.

It is believed that atomic hydrogen is the drive behind all the gas phase (plasma) chemistry during the deposition of diamond thin films [53,54]. In the hot regions, atomic hydrogen abstracts hydrogen atoms from methane molecules, creating radicals which can recombine into C_xH_y species containing two or more carbon atoms. The conversion between C_1H_y and C_2H_y species is one of the reactions within the plasma that receives a lot of attention [55-57]. Since all microwave plasma reactors contain steep gradients of the gas temperature, the concentrations of the various hydrocarbon species are very sensitive functions of the location within the reactor [54]. Nowadays, laser absorption spectroscopy methods enable the probing of spatially resolved densities of hydrocarbon species [56,57].

In order to unravel the growth mechanisms of UNCD and NCD, correlations between the composition of the plasma close to the surface and the resulting film properties have been considered [58-60]. One of the most striking findings considering the gas phase chemistry during diamond growth was accomplished by means of optical emission spectroscopy and cavity ring-down spectroscopy [60]. Indeed, Rabeau et al. proved that the growth of both UNCD and NCD is independent of the C_2 radical, which was until then believed to be the major growth species of PE-CVD diamond [61]. Since then, C_1H_y species are believed to be the most important species contributing to diamond growth (see section 3.1 below). However, as some hydrocarbon species (e.g. C_2H) cannot be detected by spectroscopic means under standard plasma growth conditions [52], computer simulations become an invaluable tool to

investigate the gas phase chemistry during (U)NCD growth. Indeed, it is expected that a detailed understanding of the gas phase chemistry will be reached by complementary theoretical and experimental work [54].

A lot of modeling work on the plasma chemistry for (U)NCD plasma deposition has been carried out by May, Ashfold, Mankelevich and colleagues [52,62-65]. In [52,62-64], a 2D model was applied to calculate the gas phase composition in a hot filament (HF) and microwave (MW) plasma CVD system for (U)NCD growth. The model consists of three parts, which describe (i) the activation of the gas mixture, (ii) the gas dynamics and chemical kinetics, and (iii) the gas-surface interactions. The shape and size of the plasma ball are taken as input parameters, obtained from experiments. Also, a uniform absorbed power density and electron temperature were applied; the latter was obtained from a 0D plasma kinetics model, solving balance equations for given reduced electric fields. 35 chemical species and around 300 reactions were considered in the model. Based on these model calculations, the authors could explain why in their experiments UNCD films can be grown much more easily in the MW plasma than in the HF CVD reactor. Furthermore, the model predicts that the densities of CH_3, C and C_2H are greater than the C_2 density, suggesting that these species are more important precursors for UNCD growth [52,63]. Another 2D model was developed by the same group for a dc arc jet reactor, also used for microcrystalline diamond (MCD) and NCD deposition [65]. This model includes gas activation, expansion in the low pressure reactor chamber and reaction chemistry in the plasma and at the surface. C and CH are predicted to be the main radical species bombarding the growing (nano)diamond surface.

Gordillo-Vázquez and Albella also developed a quasi-analytical space-time-averaged kinetic model for an rf $C_2H_2/H_2/Ar$ plasma used for NCD film deposition, with special focus on the underlying mechanisms driving the nonequilibrium plasma chemistry of C_2 [66-68]. The authors suggest that the growth of NCD films under these conditions is very sensitive to the contribution of C_2 and C_2H species [67].

Finally, Hassouni, Lombardi and colleagues studied an $Ar/H_2/CH_4$ MW discharge used for NCD deposition by means of experiments and 0D plasma chemistry modeling [58,69]. The authors suggest that so-called “sp” species, especially C_2H_2, play a key role in the surface chemistry that governs the diamond growth [58]. As soot formation is often observed experimentally in this kind of plasma reactor, the mechanisms giving rise to soot particles, including both ionic and neutral pathways, were investigated in [69].

(b) CNTs and related structures

Other carbon nanostructures, such as carbon nanotubes (CNTs), carbon nanofibers (CNFs), carbon nanowalls (CNWs) and carbon nanocone arrays, can also be grown in plasmas. Low temperature PE-CVD offers even some advantages over conventional CVD growth techniques, as it results in vertical alignment and ordering of the carbon nanostructures, due to the electric fields normal to the growth surface [7,70,71]. As mentioned by Denysenko and Ostrikov [72], it is commonly accepted that the growth and structure of CNTs, CNFs and related carbon nanostructures is determined on the surface and within the metal catalyst nanoparticle. However, it remains unclear how the plasma affects these processes, and translates into higher growth rates, lower activation energies and lower growth temperatures, and this is one of the main obstacles to a deterministic plasma-aided synthesis of carbon nanostructures [72]. Also Meyyappan stated in his recent review paper the need for more modeling work on CNT PE-CVD [7].

Several modeling efforts have been presented in literature to describe the plasma chemistry in various types of plasma reactors used for carbon nanostructure growth, including dc plasmas [73-76], capacitively coupled rf plasmas [77,78], and inductively coupled plasmas (ICPs) [79-85]. These are either 0D chemical-kinetics models [79-82], 1D [73-78] or 2D [83-

85] fluid approaches. The gas mixtures considered in these models are the typical gases used for the growth of CNTs (and other carbon nanostructures), and consist of either CH_4 or C_2H_2 as hydrocarbon growth precursors, mixed with H_2 or NH_3 as etchant gases, sometimes diluted with Ar. Typical calculation results include the density profiles and fluxes of the species bombarding the growing nanostructure, i.e., the growth precursors. It is reported that C_2H_2, C_2H_4, H and CH_3 are major neutral species. Atomic H is important because it yields preferential etching of amorphous carbon phases, resulting in more "clean" CNT formation. Furthermore, the models yield also information about the conversion (also called "decomposition rate") of the feedstock gases in the plasma.

In [84] we have applied a 2D hybrid MC-fluid model, i.e., the so-called hybrid plasma equipment model (HPEM), developed by Kushner and coworkers [86], to describe the detailed plasma chemistry in an ICP reactor used for CNT synthesis in four different gas mixtures, i.e., CH_4/H_2, C_2H_2/H_2, CH_4/NH_3 and C_2H_2/NH_3. In a subsequent paper [85] a numerical parameter study was carried out with this model, varying the gas ratios, gas pressure, coil power, bias power and substrate temperature. Figure 3 illustrates the calculated conversion of the feedstock gases in each of the gas mixtures investigated, as a function of the hydrocarbon gas fraction (CH_4 or C_2H_2). As is clear from figure 3(a,b), the CH_4 conversion seems to drop from 0.7-0.8 at low CH_4 concentration in both the CH_4/H_2 and CH_4/NH_3 gas mixtures, to about 0.4 in pure CH_4. The C_2H_2 conversion drops from roughly 1 (=100%) at 5% C_2H_2 gas fraction in both the C_2H_2/H_2 and C_2H_2/NH_3 gas mixtures, to 0.1 in pure C_2H_2 (see figure 3(c,d)). Hence, at low hydrocarbon gas fraction, our calculations predict that both CH_4 and C_2H_2 are much more efficiently converted into other (reactive) growth precursors than at high hydrocarbon gas fraction or in the pure hydrocarbon gases. The calculated conversion of H_2 (see figure 3(a,c)) is very low or even negative in some cases, indicating that more H_2 is created than converted, due to dissociation of CH_4 or C_2H_2. On the other hand, the NH_3 conversion is predicted to be quite high, i.e., around 0.9 in the CH_4/NH_3 mixture (cf. figure 3(b)) and decreasing from 0.9 to 0.4 in the C_2H_2/NH_3 mixture (cf. figure 3(d)). Indeed, it was observed in the calculation results that NH_3 decomposes easily to produce atomic H, especially at low hydrocarbon gas fraction. In general, our model predicts that a lower fraction of hydrocarbon gases (CH_4 or C_2H_2, i.e., below 20%) and hence a higher fraction of etchant gases (H_2 or NH_3) in the gas mixture result in more "clean" conditions for controlled CNT growth, due to the dominant role of atomic H [85], which is in agreement with literature observations (e.g., [76,83,87-90]).

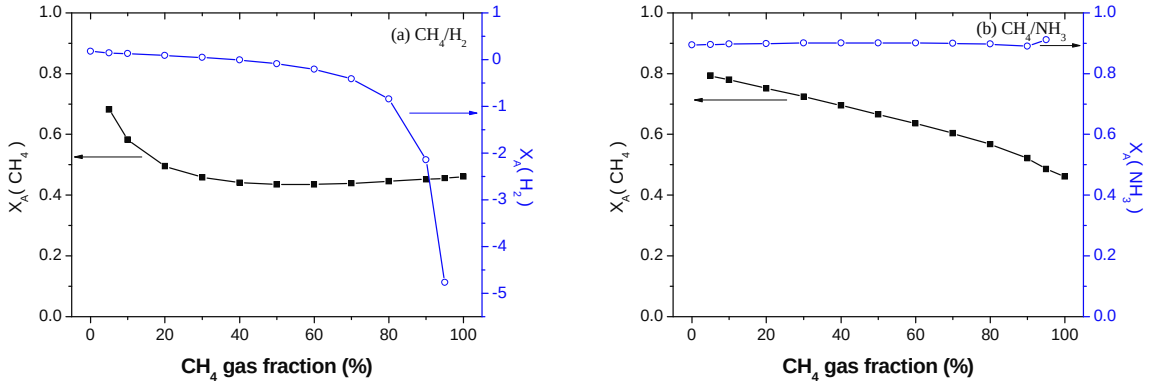

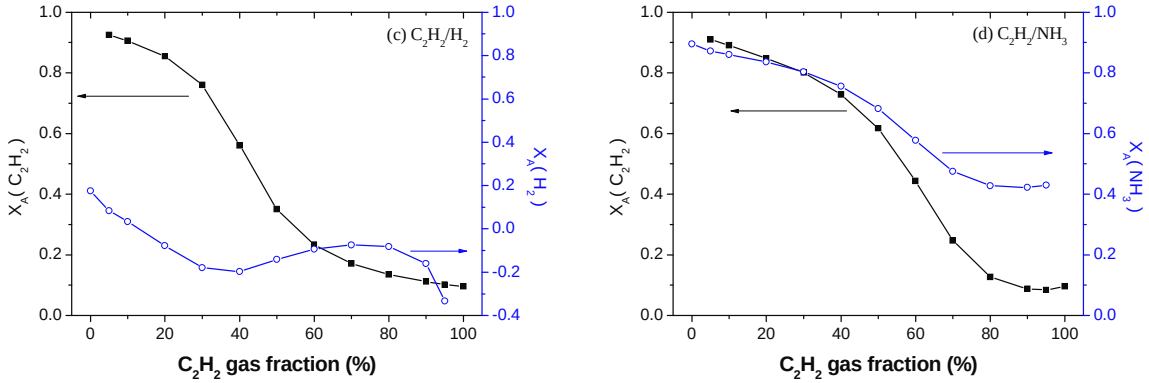

<u>Figure 3:</u> Calculated conversion (x_A) of the different feedstock gases in each of the gas mixtures investigated, i.e., CH_4/H_2 (a), CH_4/NH_3 (b), C_2H_2/H_2 (c) and C_2H_2/NH_3 (d), as a function of the hydrocarbon gas fraction (CH_4 or C_2H_2), for an ICP reactor at 50 mTorr gas pressure, 100 sccm total gas flow rate, 300 W source power, 30 W bias power and 13.56 MHz operating frequency at both the coil and the substrate electrode. The substrate is heated to 550 °C.

3. Modeling of plasma-surface interactions and the growth mechanisms of nanostructured materials

The fluxes of the various plasma species impinging on the substrate, as calculated by the plasma modeling, can be used as input for the simulations of the plasma-surface interactions and hence for describing the growth process of the nanostructured materials. Roughly, two different simulation approaches can be distinguished for describing the nanostructure growth mechanisms, i.e., an atomistic approach, providing detailed information on the interaction mechanisms of plasma species with the growing nanostructure, and a more macroscopic, phenomenological approach, which can give an overall illustrative view of the growth mechanisms. In the following, we will first explain a few of these phenomenological, mechanistic approaches presented in literature, before zooming into the detailed atomistic simulations of nanostructure growth processes, where some examples of our own research group will be given.

3.1. Mechanistic modeling of nanostructure growth processes

(a) NCD and UNCD

As mentioned above, the model developed by May, Mankelevich et al. [52,62-64] does not only describe the plasma chemistry for (U)NCD film growth, but it gives also information about the growth process itself, by mechanistic modeling. The model considers 9 gas-surface reactions, involving the H-abstraction to form surface sites, and the subsequent reactions of H and hydrocarbon radicals with these surface sites. These reactions affect the gas composition near the surface [52,64]. For the case of UNCD deposition, the renucleation mechanisms (i.e., the creation of surface defects which change the growth direction and act as a renucleation site) were discussed in detail [52]. It was stated that the measured film morphology can be rationalized based on competition between H atoms, CH_3 radicals and other CH_x species reacting with dangling bonds on the surface [64]. Further, a general mechanism for the deposition of MCD and NCD from CH_4/H_2 gas mixtures and for UNCD films from $Ar/CH_4/H_2$ gas mixtures has been proposed, which is consistent with published experimental data [64].

It should be noted, however, that the gas surface reactions included in this model involve only those for which thermodynamic and kinetic data were available, i.e., only for H, H_2, C_2H_2 and the CH_x species, and not for C_2, C_2H and higher hydrocarbon species [64]. While the simulations reach long time scales, i.e., (U)NCD growth is simulated in real time [91], this method is limited by the requirement that a complete catalogue of all relevant transitions and their rate constants has to be known in advance. Therefore, the completeness of this catalogue depends on the intuition of the scientist applying the method and the availability of the kinetic data. Furthermore, not all transition mechanisms are known. Indeed, in [91], May et al. list the questions that raise during the construction of the catalogue.

More information on these surface reaction data can, however, be obtained from detailed atomistic descriptions, such as molecular dynamics (MD) simulations. MD simulations are computationally more expensive, but they allow to investigate the evolution of the system without any assumptions regarding (reaction) mechanisms (see below).

(b) CNTs and related structures

Several research groups have published mechanistic models for obtaining a better understanding of the growth mechanisms of CNTs (and related nanostructures). They are all more or less based on the same processes, including adsorption and desorption of carbon species at the metal catalyst particle, surface and bulk diffusion, surface reaction on the catalyst and substrate, and nanostructure nucleation and growth. Most of these models are applied to CNT growth by CVD, but some are applied also for PE-CVD, and in general the principles are the same for both growth techniques.

Table 1 summarizes the different mechanistic growth models published in recent years, indicating the processes included in each model, the reactor type (CVD or PE-CVD) and the simulation method. From this overview it is clear that the mechanistic models can be divided into three groups from simulation point of view, i.e., kinetic models [92-99], multiphysics, multiphase integrated models [100-103] and kinetic Monte Carlo (MC) models [104-107].

Table 1: Overview of the different mechanistic growth models for CNTs, presented by different groups

Reference	Growth Process				Simulation Method	Reactor Type
	Adsorption and desorption of carbon species	Surface diffusion and bulk diffusion	Surface reactions (H abstraction, radical recombination,...,)	Nanostructure nucleation and growth		
92	Yes	Yes	No	Yes	Kinetic model	CVD
93	Yes	Yes	Yes	Yes		CVD
94	Yes	Yes	Yes	Yes		CVD
95,96	Yes	Yes	No	Yes		CVD
97,98	Yes	Yes	Yes	No nucleation		PECVD
99	Yes	Yes	Yes	Yes		CVD
100	Yes	No bulk diffusion	Yes	Yes	Multiphysics multiphase integrated model	CVD
101,102	Yes	No bulk diffusion	Yes	Yes		
103	Yes	No bulk diffusion	Yes	Yes		
104-107	Yes	Yes	No	Yes	Kinetic MC	PECVD

Puretzky and co-workers [92] presented a kinetic model for the CVD-based growth of vertically aligned nanotube arrays (VANTAs) from C_2H_2, based on *in situ* measurements.

Besides the processes mentioned above, the gas-phase decomposition of C_2H_2 and the formation of pyrolysis products in the gas phase, as well as the additional growth of the carbonaceous layer due to these gas-phase pyrolysis products and the catalyst deactivation, were also included. Each process was described by a single rate constant in an Arrhenius form. The role of the metal catalyst nanoparticles in VANTA growth, and the optimum size and composition of the catalyst nanoparticles for the fast growth of long and dense VANTAs were analyzed. The simulated results fitted the measurements very well. This model was recently further improved by Lee and co-workers [93] by including an additional description for the dependence of the termination length on the size of the catalyst particles and the wall number of CNTs. A parametric study showed that the simple kinetic model can successfully predict the kinetics of CNT growth [93].

A kinetic model of CH_4 decomposition and filamentous carbon formation on supported Co catalysts was developed by Zhang and Smith [94]. The geometry of the catalyst particles was considered and approximated as a slab with height of 2/3 d_p in the model, where d_p denotes the average diameter of a catalyst particle. The model results showed that the Co particle size played an important role in the CH_4 decomposition activity. This model was later on improved by Naha *et al.* [95] and applied to the flame synthesis of CNTs and CNFs.

A more detailed kinetic model [96] was developed by Naha and Puri, based on the models of [92,94,95]. The model included the impingement of C atoms, their adsorption and desorption on the catalyst surface, surface and bulk diffusion, and nucleation and separation of solid C in nanostructured form. The model was validated by experiments, and subsequently a parametric study was presented. The model predicts a rise of the CNT length with temperature and feedstock gas partial pressure, consistent with previous experiments [96].

The model by Denysenko and Ostrikov [97,98] for the PECVD of CNFs also accounts for adsorption and desorption of C_2H_2 and H, surface and bulk diffusion, incorporation into a graphene sheet, as well as ion- and radical-assisted processes on the catalyst surface that are unique to a plasma environment. It is shown that plasma ions play a key role in the carbon precursor dissociation and surface diffusion, enabling a low-temperature growth of carbon nanostructures. In [98], the plasma heating effects were considered. The authors found that the calculated growth rates were in better agreement with the available experimental data than the results without heating effects.

Finally, a phenomenological kinetic model was recently developed by Latorre *et al.* [99], which included all the relevant steps involved in the CNT growth by catalytic CVD, including carbon source decomposition, nanoparticle surface carburization, carbon diffusion, nucleation, CNT growth, and growth termination by catalyst deactivation or by the effect of sterical hindrance. The model was applied to fit data obtained by experiments, and the values obtained for the kinetic parameters have a realistic physical meaning, in good agreement with the mechanism of CNT formation [99].

In order to establish relationships between the fabrication process parameters and the growth conditions for CNTs in CVD, a multiphysics, multiphase integrated model has been developed by several groups [100-103]. In these models, all processes of CNT growth are represented by a series of surface reactions. These models bridge the gap between the reactor and molecular length scales.

Grujicic *et al.* [100] developed a coupled boundary-layer laminar-flow hydrodynamic, heat-transfer, gas-phase chemistry and surface chemistry model to analyze CNT growth by CVD in the presence of Co catalytic particles. Optimization of the CNT fabrication process identified the optimum processing parameters which gave rise to a trade-off between two objectives: to maximize the overall carbon deposition rate as well as the amount of carbon deposited as nanotubes.

Lysaght and Chiu reported on a coupled gas phase and surface chemistry model for the CVD of CNTs, based on conservation of mass, momentum and energy equations in combination with gas-phase and surface chemical reactions [101,102]. The latter are based on adsorption and desorption of the reactive species to and from active sites, hydrogen abstraction from surface bound hydrocarbons, as well as diffusion from the active site toward the nanotube growth edge. The limiting reaction steps for the surface chemistry were identified and the optimum process conditions for efficient CNT production were discussed.

Hosseini et al. presented a time-dependent multiphysics, multiphase-based model [103] for the CVD-based CNT fabrication process in CH_4-H_2 mixtures. The different synthesis conditions were studied. They found that the main role of H_2 gas species during the CNT fabrication process is to reduce the formation of other undesirable forms of carbon structures, such as amorphous carbon.

Finally, Levchenko, Ostrikov and colleagues [104-107] presented an interesting multiscale MC/surface diffusion model for the plasma-based growth of carbon nanocone arrays on metal catalyst particles. The model comprises the three main physical phenomena that play a key role in the nanostructure formation, i.e., (i) diffusion of adsorbed carbon atoms on the substrate surface toward the metal catalyst nanoparticles, (ii) dissolution into the nanoparticle and eventually saturation of metal catalyst with carbon, resulting in nanocone nucleation and growth on top of the catalyst particle, and finally (iii) sputtering of the carbon nanocone with impinging carbon ions from the plasma. These processes are schematically illustrated in figure 4. The model predictions suggest that the plasma parameters can effectively tailor the nanocone array properties and ultimately increase the array quality [106].

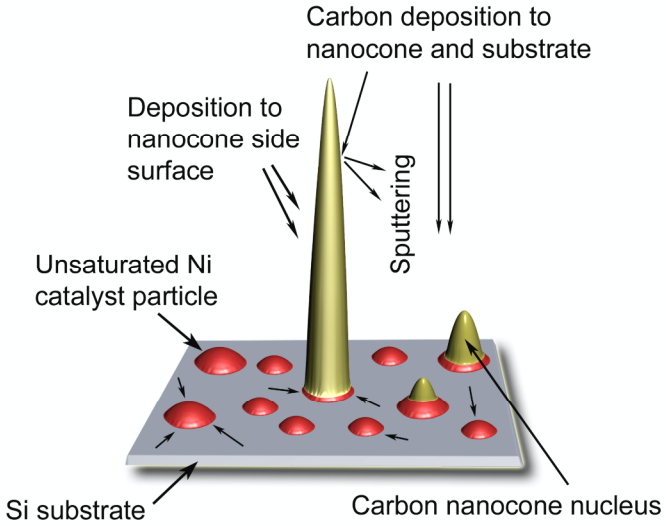

Figure 4: Schematic diagram of the processes considered in the simulation of nanocone array formation by Levchenko et al. Reprinted with permission from [106]. Copyright 2008, American Institute of Physics.

In general it can be concluded that kinetic simulations are particularly attractive because of their simplicity and minor computational effort. In a kinetic simulation, all possible processes are described either with diffusion coefficients (for diffusion processes) or with rate constants (for reactions). Based on these parameters a set of continuity equations is solved as a function of time, allowing to predict the time-dependent growth rate and length of the CNTs, and the influence of processing parameters on these quantities. The multphysics, multiphase models are based on the same principles, but they are integrated in a reactor model (for CVD) or a plasma model (for PE-CVD), to obtain self-consistent calculations. However, in this approach it is typically not so straightforward to express bulk diffusion processes.

On the other hand, in kinetic and related models, the diffusion coefficients of growth precursors and the rate constants for the reactions have to be introduced as input; they need to be obtained either from experiments or from detailed atomistic simulations (see below), as was also explained above for the (U)NCD growth. Moreover, kinetic models cannot predict the atomic structure of the growing CNTs. For this purpose, atomistic simulations need to be applied, as will be illustrated in the next section.

3.2. Detailed atomistic simulations of nanostructure growth processes

As mentioned above, the mechanistic modeling can be very instructive to obtain more insights in the growth processes, but it provides a more qualitative picture, and it depends strongly on the availability and correctness of reaction rate coefficients and activation energies of the many processes involved. It should be realized that these energies are most likely different for nanostructures as compared to bulk materials. The input data for mechanistic modeling, such as reaction rate coefficients and/or activation energies, can be obtained by ab initio (i.e., first principles) methods or by classical MD simulations.

In solid state physics, one of the most popular first principles methods is the density functional theory (DFT). Within DFT, the energy of the investigated system is completely determined by the electronic charge density. DFT allows the calculation of the energy of many-body systems, and enables therefore the search for their energetically most probable configuration. In order to find probable reaction mechanisms of (U)NCD, DFT calculations have been applied by various scientists [61,108-111]. By applying DFT and tight binding (TB) DFT calculations, the C_2 radical when stuck to the diamond (100) surface was predicted to play a major role in the re-nucleation during UNCD growth, i.e., the formation of new diamond nuclei that evolve into diamond crystallites [112,113]. The latter was, however, disproved by Rabeau et al. [60], as mentioned above. Besides the C_2 radical, also the methyl radical has been investigated extensively by means of DFT, that is, the carbon incorporation through CH_3 into dimers of the diamond (100) surface [108,109]. Based on these calculations, the CH_3 radical is the main species contributing to diamond growth within the 'standard growth mechanism' of diamond [54].

Although in the study of (U)NCD, DFT calculations provide very valuable information about probable reaction mechanisms, the DFT calculation time is reasonable for systems containing at maximum only about 100 atoms. In order to extend the length scale of first principles calculations, hybrid quantum-mechanical–molecular mechanics (QM/MM) methods have been developed [114,115]. In QM/MM, the essential part of the system (i.e., the atoms that are involved in the investigated reaction) is treated by means of e.g. DFT, and the surrounding atoms by means of classical dynamics. QM/MM calculations confirm the prominent role of the CH_3 radical in the standard growth mechanism of diamond [114,115].

In contrast to (U)NCD growth, DFT-based MD calculations are rather rare for CNT growth. The first of such studies was carried out by Gavillet et al. [116]. In this simulation, a cluster consisting of 153 atoms (carbon and cobalt) was cooled down from 2000 K to 1500 K in 5 ps. It was found that most of the carbon was deposited on the surface, with the formation of surface chains and some aromatic rings. In the same paper, the authors also investigated the incorporation of C into a pre-formed fullerene cap attached to a cobalt surface [116]. The incorporation of C_2 fragments to a pre-formed cap with defined chirality was investigated by Gómez-Gualdrón et al. [117]. Using a grand canonical MC simulation, Amara et al. [118] investigated the nucleation of carbon caps on small nickel nanoparticles. A tip growth mechanism was demonstrated by Charlier et al. [119]. Actual growth and elongation of a SWNT on a small metallic particle was achieved using DFTB simulations by Ohta et al. [120,121].

As mentioned before, DFT simulations are usually limited to about 100 atoms. While simplified approaches, such as DFTB, alleviate this restriction, both the number of atoms and the attainable time scale remain 1 or 2 orders of magnitude smaller than what can be achieved with classical MD. Therefore, whereas quantum mechanical calculations provide valuable kinetic data and they have a decreasing computational cost (due to cheaper and faster processors), MD simulations are believed to continue playing an important role for the exploration of unknown reaction mechanisms [122]. After the discovery of possible reaction paths, an investigation at higher level of theory might then be appropriate.

In classical MD simulations, the movement of all the atoms in the system is calculated as a function of time by Newton's laws, where the force is obtained as the negative derivative of the interatomic interaction potential. Hence, it is a deterministic method, which does not depend on *a priori* assumptions, in contrast to the mechanistic models. However, the reliability of the classical MD calculations strongly depends on the quality of the interatomic interaction potential. In our research group, we make use of the Brenner potential for hydrocarbons [123] for describing (U)NCD growth. For CNT growth, the interaction with the metal catalyst particle needs to be accounted for, which is not included in the Brenner potential. Therefore, we use the ReaxFF potential, developed by van Duijn [124]. In this potential, the total system energy is a sum of several partial energy terms; these include energies related to lone pairs, under-coordination, over-coordination, valence and torsion angles, conjugation, hydrogen bonding, as well as van der Waals and Coulomb interactions. Because Coulomb and van der Waals interactions are calculated between every pair of atoms, the ReaxFF potential describes not only covalent bonds but also ionic bonds and the whole range of intermediate interactions. Furthermore, as the REAXFF potential takes polarization into account, it should be able to describe CNT growth in a charged environment such as plasmas, where polarization effects are caused by non-uniform microscopic distributions of charges and fields in the vicinity of nanostructures (see [125]).

In the following, we will first focus on MD simulations for (U)NCD growth, from literature and from our research group. Also the coupling with Metropolis MC (MMC) calculations, needed to handle the longer time scale behavior of surface relaxation, will be briefly explained. Subsequently, CNT growth simulations by MD (and combined MD-MC) will be reviewed, again both from literature and from our own research group.

(a) NCD and UNCD

The interaction between impacting hydrocarbon species and (nano)diamond surfaces has been investigated by MD simulations, since this technique takes the dynamics of the system into account. The interaction of CH_3 and C_2H_y species with diamond (100) and (111) surfaces has been studied extensively by several scientists [126-128]. The simulations by Träskelin et al. have been performed for an improved insight into the erosion of hydrogenated carbon-based films under ITER-relevant conditions [127,128]. Nevertheless, the simulation results, including the finding that the sticking process depends on the angle of incidence and the local atomic neighborhood of the impacted reactive site [127], are also valuable for understanding the growth of (nano)diamond. Zhu et al. identified different chemisorption configurations, among which the cross-linking between two neighboring reactive sites, when examining the behavior of C_2H_2 molecules impacting diamond (100) surfaces [126]. Cross-linking describes the sticking of two carbon atoms of the impacting C_xH_y species to two different surface sites. Analogous configurations were found for C_2H_2 impacting diamond (111) surfaces [128].

A very detailed study of the chemisorption probabilities, i.e., the sticking coefficients, and the configurations of various C_xH_y species at both diamond (100) and (111) surfaces was carried out by Eckert et al. [129,130]. The sticking coefficients of the relevant growth species

for the microwave enhanced PE-CVD of both NCD and UNCD (i.e., CH_x (x=0-4), C_2H_x (x=0-6), C_3H_x (x=0-3) and C_4H_x (x=0-2)), on the two most important crystallographic diamond surfaces were calculated. For this purpose, MD simulations were carried out at two different substrate temperatures, typical for UNCD and NCD. It was found that the sticking efficiency depends on both the number of free electrons and hydrogen atoms of these species [129], very similar to the observations by Träskelin et al. when studying the behavior of C_2H_y species impacting diamond (111) surfaces, published almost at the same time [128]. Furthermore, a higher substrate temperature promotes higher adatom coordination, which is required for the growth of diamond structures. This might explain why larger diamond crystals, as typical for NCD, can be grown at higher temperature, whereas UNCD, with its high percentage of disordered phases, is grown at lower substrate temperature. Also the different bonding structure of the two surfaces (i.e., diamond (100)2x1 and diamond (111)1x1) causes different temperature effects on the sticking efficiency. It was found that diamond (111) growth is promoted by a higher temperature above diamond (100), which was found in correlation with experiments [130]. Finally, based on the calculated sticking coefficients, in combination with the plasma chemistry simulation results from May et al. [52] for the species concentrations above the growing diamond film, it was suggested that, within their series, C, C_2H_2, C_3 and C_4H_2 are the most important growth species for UNCD growth, whereas CH_3, C_2H_2, C_3H_2 and C_4H_2 are predicted as the major growth species for NCD growth [130].

MD simulations do not only provide information on the sticking coefficients, or more in general, on the surface reaction probabilities, but they can also give more insight in the detailed growth mechanisms of nanostructured materials. Probably the most famous publication concerning reaction mechanisms at diamond surfaces, was written by Garrison et al. in 1992 [131]. Applying the Brenner potential, the reaction mechanism of dimer opening at the diamond (100)2x1 surface and subsequent insertion of CH_2 was discovered, by means of MD simulations. Based on these findings, investigations at higher level of theory were carried out, among which DFT calculations (see above). Until now, this reaction mechanism is believed to be the essential part of the standard growth mechanism of diamond (see above).

A number of processes that is relevant for the evolution of thin film growth, e.g. relaxation processes and diffusive events, however, take place at the microsecond time scale. Consequently, those processes can hardly be simulated by means of MD. In order to overcome the “time-scale problem” of MD simulations, different MC methods have been designed. In contrast to the deterministic MD simulations, MC simulations are probabilistic, and computationally less demanding. One famous example is the MMC algorithm, which was developed in the 1950's [132]. In MMC, no activation barriers are taken into account. The system is allowed to evolve based on thermodynamic properties of the system. Within an MMC simulation, the system evolves by random displacements (“moves”) of the atoms and clusters of atoms. Depending on the energy change caused by this random displacement, the move is accepted or rejected. This sampling is performed by applying the Boltzmann distribution function, i.e., samples of a canonical ensemble (or "NVT ensemble") are generated. In essence, the Metropolis method is a Markov process in which a random walk is constructed.

For the (U)NCD films, Eckert et al. have demonstrated by means of combined MD – MMC simulations, how the diamond structure is pursued on the atomic level and at longer time scale [133-135]. When stuck to flat diamond surfaces, it was shown that C_xH_y species with $x \geq 2$ do affect the growth of the diamond films, in contrast to the assumption that only C_1H_y species contribute to the growth of nanostructured diamond, as proposed in the standard growth mechanism of diamond [54]. For instance, for both UNCD and NCD, C_2H_2 and C_3H_2 are important species that pursue the diamond lattice with a high probability [134]. In figure

5, an example is shown of how a carbon atom and an acetylene molecule can pursue the diamond structure when stuck to the diamond (111) surface.

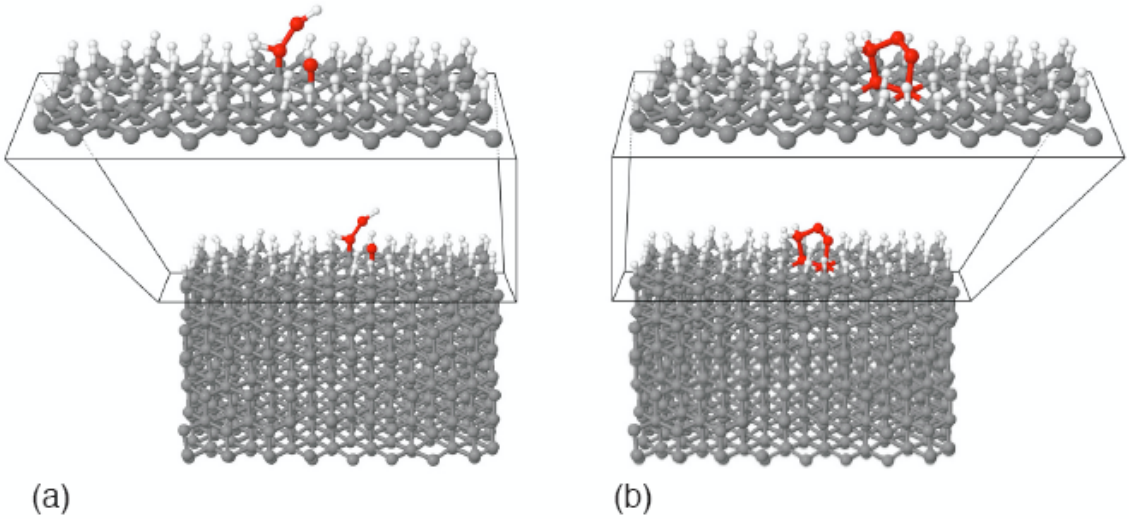

Figure 5: Side view of the input (a) and final (b) configuration of a MMC simulation. The white and gray spheres indicate hydrogen and carbon atoms, respectively. The input simulation is obtained by an MD simulation of an impacting carbon atom and an impacting C_2H_2 molecule; their carbon atoms are marked red. In the final configuration, one can observe the formation of a new carbon six ring (marked by red spheres), which proves that the diamond crystal structure is pursued.

The same conclusions were drawn when the longer time scale behavior of C_xH_y species at the so-called “step edges” delimiting diamond terraces were investigated [135]: C_2H, C_2H_2 and C_3H_2 all have a high reactivity, implying a prominent role during the growth of (U)NCD. Indeed, e.g. C_2H has a high density above the growing NCD surface (see section 2.2) [52,63]. This confirms the recent doubts that the C_1Hy species are the only important growth species of (U)NCD [136].

Furthermore, the MD-MMC simulations of C_xH_y species at diamond step edges have elucidated the different growth regimes of UNCD and NCD [135]. Crystal growth through the extension of the step edges, the so-called "step flow growth mechanism" is believed to result in well-faceted, smooth diamond films [137]. Indeed, during the growth of NCD films, the species that are found to contribute to the step flow growth mechanism, are generally accepted to be important for NCD growth [135]. In other words, the species present above the growing NCD film enhance the step flow growth mechanism, resulting in the well-faceted morphology that is characteristic for NCD films. For UNCD, however, the species that cause the formation of defects at the step edges, are generally considered to be important for UNCD growth [135]. The absence of the step flow growth mechanism during UNCD growth therefore explains the non-faceted morphology and the characteristic high fraction of non-crystalline phase within the UNCD films.

(b) CNTs and related structures

One widely accepted model for CNT growth is the so-called “vapor-liquid-solid” model, which was originally put forward to explain the growth of silicon whiskers by Wagner et al. [138] and later on applied to CNFs by Baker et al. [139]. In this model, the vapor carbon source is assumed to dissolve into a liquid (metal) catalytic particle, thereby forming a metal carbide. Upon supersaturation, the carbon starts to precipitate from the liquid, forming a solid fiber or tube. However, to explain the low-temperature PECVD growth, at temperatures

below the melting point of the catalytic particles, a surface-mediated carbon transport model was proposed by Helveg et al. [140]. While the formation of an eutectic alloy is required in both of these mechanisms, single-walled CNTs (SWNTs) are also observed to grow on non-metallic nanoparticles which do not form an eutectic alloy [141]. Examples include diamond, Si, SiC and alumina. Here, the CNT is believed to nucleate on a sp^2 carbon surface layer, covering the nanoparticle.

The first classical MD simulations on the growth of CNTs were performed by Maiti et al. [142,143]. The C-C interactions were described by the Brenner potential, while the metal atoms were not explicitly taken into account. Rather, the authors used a repulsive cylinder, around which the SWNT could grow.

The first MD simulations taking into account the metal atoms were carried out by Shibuta et al. [144]. The C-C interactions were described based on a simplified Brenner potential, while parameters for C-metal and metal-metal interactions were fit to DFT energies of small clusters. The catalytic CVD process was simulated by allowing C-atoms to impinge on small nickel clusters (Ni_{32}, Ni_{108} and Ni_{256}) at 2500 K. In the total simulation time of 130 ns, a cap structure was formed, which subsequently lifted off from the surface of the cluster [145]. The same authors also investigated the effect of the substrate on the catalytic particles during SWNT growth [146]. It was found that in the case of strong cluster-substrate interaction, a layered metal structure and a graphene layer parallel to the substrate were formed. In the case of weak metal-substrate interaction, the metal did not adopt a specific orientation, and the graphene sheet separated from the cluster in a random direction.

Balbuena and co-workers have developed an updated version of the Shibuta potential [147] and presented a step-by-step overview of the observed processes in the simulation during SWNT growth [148]. Very recently, Ribas et al. [149] used this potential to investigate the effect of the adhesion strength of the graphitic cap to the catalyst and of the temperature on the SWNT growth. It was found that at high temperature (>600 K), catalyst encapsulation depends on the work of adhesion, while at lower temperature, limited carbon diffusion hinders cap formation and cap lift off. Furthermore, they succeeded in reaching the stage of actual tube elongation, beyond cap formation only, up to a length of 13 nm.

Ding et al. performed a series of simulations probing the influence of various parameters and growth conditions on the growth mechanism. The growth mechanism was found to shift from bulk diffusion mediated to surface diffusion mediated at around 900 K – 1000 K [150]. Larger clusters resulted in an enhanced growth of SWNTs compared to smaller clusters (<20 atoms). Moreover, in agreement with the experiment, it was also found that clusters with diameters smaller than 0.5 nm yield tubes with slightly larger diameters of 0.6 – 0.7 nm [151]. Also the effect of temperature gradient was investigated by this group [152,153], concluding that while a temperature gradient may be important for larger particles, it is not required for SWNT growth from small particles.

It should be realized, however, that all of these simulations employ a carbon addition rate to the cluster in the order of 1 particle per 50 ps or faster. This is much higher than the actual addition rate and therefore these simulations do not include relaxation effects. To extend the timescale of MD simulations in order to take such relaxation effects into account, so-called accelerated MD simulations (such as hyperdynamics, parallel replica or temperature accelerated dynamics) can be applied [154]. However, Neyts et al. have recently shown that the fundamental dynamics in the carbon-nickel system at SWNT growth temperatures are too fast to directly apply accelerated MD techniques [155]. Alternatively, deterministic MD simulations can be coupled to stochastic MC simulations, for instance uniform-acceptance force biased Monte Carlo (UFMC) [156-158] allowing to take into account relaxation effects, albeit at the price of loosing time information. Recently, Neyts et al. have successfully applied

a hybrid MD/UFMC approach for the simulation of the melting mechanisms of nickel nanoclusters [158].

This methodology can also be succesfully applied to the growth of SWNTs [159]. In figure 6, two carbon caps protruding from a small Ni-cluster can be seen, together with some amorphous material.

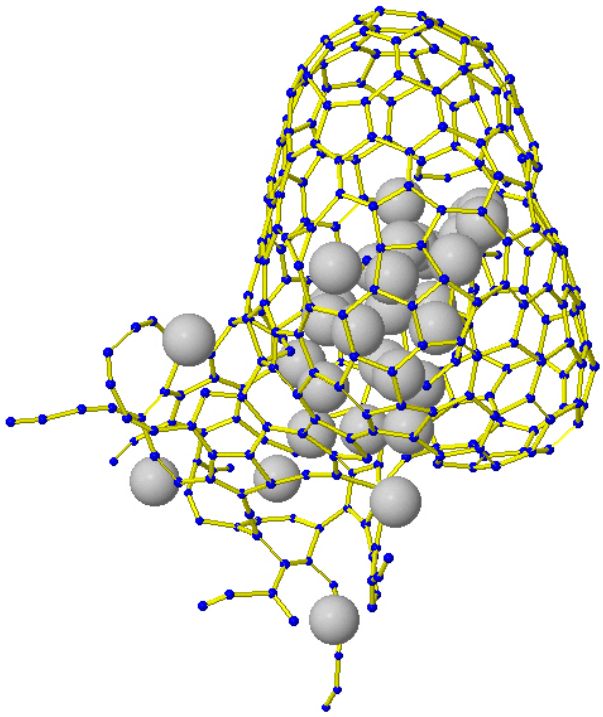

Figure 6: Calculated $Ni_{32}C_{311}$ structure. Ni is represented by the larger grey balls, and carbon is represented by the smaller blue balls. This structure was generated by alternating MD and MC cycles as described in the text.

This structure was generated as follows. Every 2 ps, a carbon atom was allowed to impinge on the Ni_{32} cluster. To prevent atomic carbon from adding directly to the already deposited carbon material, a repulsive potential was put in place, such that the carbon can only react at the metallic surface. The temperature was set to 1200 K. After every second impact, the total structure was allowed to relax using the UFMC algorithm. Then, another 2 impacts were performed, and so on.

Various stages could be distinguished during the growth process. After the first alloying and subsequent supersaturation stage, the first rings start to appear on the surface. Long carbon chains present on the surface rearrange themselves with the formation of new rings, leading to the formation of graphitic islands. Finally, these islands can coalesce and form a graphitic cap, which can subsequently lift off from the surface of the metal cluster. It is worth to mention that during the growth, the metal-mediated healing of defects is observed. This finally leads to the growth of a cap with a definable (12,4) chirality [159].

It is important to note that when the UFMC model is not coupled to the MD model, i.e., when relaxation effects are not included, no cap formation, but only the formation of an amorphous phase, is observed. This demonstrates the importance of taking into account relaxation effects during SWNT growth simulations.

4. Conclusions

This paper presents different modeling efforts for describing the plasma chemistry and the plasma-based growth mechanisms of silicon and (especially) carbon nanostructured materials. The first section deals with plasma chemistry modeling. The most suitable approaches for this purpose are 0D chemical kinetics modeling, (1D or 2D) fluid modeling, and hybrid MC-fluid simulations, as these approaches can take into account a rich plasma chemistry without too much computational effort. It is explained how nanoparticle formation and growth in silane and acetylene discharges can be simulated. Subsequently, a literature overview is given on the plasma chemistry modeling in hydrocarbon-based gas mixtures, used for the growth of carbon nanostructured materials, such as (U)NCD and CNTs. For the latter application, some calculation results from our own research group are presented. Such plasma chemistry modeling can provide useful information on the precursors for nanostructure formation.

The second part of the paper deals with the simulation of the (plasma-based) growth mechanisms for (U)NCD and CNTs and related structures. Several papers in literature report on mechanistic modeling, which gives an overall, albeit qualitative, picture of the growth mechanisms. Moreover, the mechanistic modeling can be combined with plasma chemistry modeling, as illustrated e.g., in [72,106]. In this approach, results from the plasma simulations, such as the fluxes of species arriving at the substrate, are used as input for the mechanistic surface models, and vice versa, the plasma-surface interactions provide boundary conditions for the plasma simulations. In this way, an integrated picture of the plasma-enhanced growth of nanostructured materials is possible. However, it needs to be mentioned that these mechanistic models depend strongly on the availability of reaction rate coefficients. The latter need to be obtained from experiments, or they can be extracted from detailed atomistic simulations, such as DFT and classical MD simulations, which are the alternative approach for studying the growth mechanisms.

DFT simulations provide very detailed and accurate information, but they are limited to very small systems and timescales (i.e., in the order of 100 atoms for a few picoseconds). Classical MD simulations can deal with larger systems (i.e., thousands to even millions of atoms) and somewhat longer timescales, especially when combined with MC simulations to treat the (longer timescale) surface relaxation processes. However, the quality of these MD simulations strongly depends on the reliability of the interatomic interaction potential used. We have illustrated some examples of classical MD-MC simulations carried out in our research group, both for (U)NCD and CNTs. It is clear that these simulations can provide a detailed insight in the growth process, without making any *a priori* assumptions, in contrast to the mechanistic models. However, the classical MD simulations suffer also from long calculation times, so in practice, they are limited to study only certain aspects of the growth process, and they cannot yet be integrated in plasma chemistry simulations. One of the main obstacles is indeed the completely different time and length scales of the processes. For instance, the plasma reactor has dimensions of several cm to m, whereas the nanostructure growth processes take obviously place at the nm-scale. Similarly, the plasma dynamics typically occur on the ns-timescale (cf. the plasma frequency) whereas the nanostructure growth rate, including structure relaxation, is typically in the order of (a few) nm/s [7].

5. Outlook and challenges

We can identify several challenges for future research on the plasma-enhanced growth of nanostructured materials. Currently, the complete growth process of nanostructured materials, such as (U)NCD and CNTs, can be investigated theoretically only by mechanistic modeling, which is clearly an approximation and has certain limitations, as explained above (e.g., the need for accurate input data). However, a modeling approach *on the atomic scale*

that is capable of simulating the complete growth process would provide a better insight into the growth of nanostructured materials.

For (U)NCD, such a model could answer how diamond films actually grow and how the plasma chemistry affects the resulting film morphology. To achieve this, MD simulations should be combined with for instance a kinetic MC model. For the latter, a very detailed catalogue of possible reaction mechanisms at the surface needs to be developed with the highest accuracy (hence: by quantum mechanical investigations). Indeed, nowadays the reaction behavior of C_1H_x species seems to be known in sufficient detail. Nevertheless, one can not be sure that only C_1H_x species contribute to the growth of (U)NCD (as was demonstrated by our MD simulations; see above). Therefore, unraveling the reaction mechanisms of stuck hydrocarbon species with two or more carbon atoms, should be the main focus of quantum mechanical investigations for (U)NCD.

For CNT growth, the combination of MD and MC simulations will also be needed for modeling the complete growth process. Indeed, from the above mentioned results (cf. figure 6) it is obvious that taking into account relaxation effects in the simulation of the growth of CNTs is crucial. One major challenge in this area is, like discussed also above for the (U)NCD growth, to go one step beyond: to effectively increase the physically simulated time, including also the kinetics of the relaxation processes during the growth. This will also bring simulation and experiment closer to each other.

Another challenge, specifically for the plasma-based growth of CNTs, is to take into account charging and polarization effects. These effects are likely to be of crucial importance, yet they are usually omitted in atomic scale simulations. Including these effects will therefore result in more realistic calculations.

Clearly, in order to fully understand the growth process, computer modeling and experiments should go hand in hand. As a modeling group, we have some recommendations for experimental research, in order to make further progress in this field. For instance, for a correct description of the plasma-surface interactions, the fluxes of the plasma species towards the growing nanostructure need to be known. They can be obtained from plasma simulations, but for instance in the case of the (U)NCD research, the measured plasma concentrations of hydrocarbon species close to the growing (U)NCD film are typically used as input. However, the densities might not be representative for the fluxes, as a high concentration of species might be the result of a low sticking probability, and therefore these species have a limited contribution to film growth. Therefore, the relative fluxes of various hydrocarbon species are requested. For that purpose, in our opinion more detailed experimental efforts (e.g., in-situ measurements) should be done.

Second, simulations are often bounded/restricted to “simple” systems, e.g. in the growth of CNTs, to atomic carbon impacts (instead of hydrocarbons), single-element catalysts (instead of alloys), limited sizes (e.g. 2 nm catalysts instead of 10 nm catalysts),… Hence, bringing simulation and experiment closer together requires an effort on both sides: simulators must develop models and algorithms to handle more complex conditions and/or develop faster algorithms, while experimentalists must design experiments to be as simple as possible, in order to be useful for verifying the computer simulations.

Finally, transmission electron microscopy (TEM) is a very useful technique for studying nanostructured materials, such as CNTs. However, currently most TEM studies on the growth of CNTs are ex-situ, i.e., the sample is removed from the growth chamber and subsequently transferred to be examined with TEM. This transfer is likely to change the structure of the generated material. It would therefore be highly beneficial to use in-situ TEM: in that way, the growth process could be studied experimentally on the atomic level *during the growth*.

To conclude this paper, in order to fully understand the growth process from a theoretical point of view, a multi-level simulation setup is needed, ranging from atomic (i.e., quantum mechanical and classical MD) simulations to macroscale simulations. Even if coupled MD and plasma simulations might not be possible in the near future because of the different time and length scales, a more loosely coupled modeling approach would be possible, where the output of classical MD simulations (i.e., surface reaction probabilities but also detailed insights in the importance of certain growth mechanisms) serves as input for the other models. In our opinion, the ultimate approach for describing the plasma-enhanced growth of nanostructured materials would be a combination of detailed MD simulations, mechanistic surface growth modeling and plasma chemistry modeling.

Acknowledgments

The examples given in this paper for the modeling work from our own research group have been realized with the financial support from the Fund for Scientific Research-Flanders (FWO), the Institute for Promotion of Innovation through Science and Technology in Flanders (IWT) and the Federal IAP-VI program.

References

1. Ostrikov K 2005 *Rev. Mod. Phys.* **77** 489-511
2. Ostrikov K 2009 *Vacuum* **83** 4-10
3. Ostrikov K 2007 *IEEE Trans. Plasma Sci.* **35** 127-136
4. Nozaki T, Ohnishi K, Okazaki K and Kortshagen U 2007 *Carbon* **45**, 364-374
5. Levchenko I, Ostrikov K, Keidar M and Xu S 2005 *J. Appl. Phys.* **98** 064304
6. Levchenko I, Ostrikov K, Keidar M and Xu S 2006 *Appl. Phys. Lett.* **89** 033109
7. Meyyappan M 2009 *J. Phys. D: Appl. Phys.* **42** 213001
8. Bouchoule A (ed) 1999, *Dusty Plasmas: Physics, Chemistry and Technological Impacts in Plasma Processing* (Wiley, Chichester)
9. Selwyn G S, McKilltop J S, Haller K L and Wu JJ 1990 *J. Vac. Sci. Technol. A* **8** 1726-1731
10. Longeaud C, Kleider J P, Roca i Cabarrocas P, Hamma S, Meaudre R and Meaudre C 1998 *J. Non-Cryst. Solids* **227-230** 96-99
11. Mangolini L, Thimsen E and Kortshagen U 2005 *Nano Lett* **5** 655-659
12. Boufendi L, Stoffels W and Stoffels E 1999 *Diagnostics of a dusty plasma, in: Dusty Plasmas: Physics, Chemistry and Technological Impacts in Plasma Processing*, Bouchoule A (ed) (Wiley, Chichester), pp 191-303
13. Bouchoule A, Plain A, Boufendi L, Blondeau J Ph and Laure C 1991 *J. Appl. Phys.* **70** 1991-2000
14. Boufendi L and Bouchoule A 1994 *Plasma Sources Sci. Technol.* **3** 262-267
15. Hollenstein Ch, Dorier J-L, Dutta J, Sansonnens L and Howling A A 1994 *Plasma Sources Sci. Technol.* **3** 278-285
16. Howling A A, Sansonnens L, Dorrier J-L and Hollenstein Ch 1993 *J. Phys. D: Appl. Phys.* **26** 1003-1007
17. Choi S J and Kushner M J 1993 *J. Appl. Phys.* **74** 853-861
18. Gallagher A 2000 *Phys. Rev. E* **62** 2690-2706
19. Gallagher A, Howling A A and Hollenstein Ch 2002 *J. Appl. Phys.* **91** 5571-5580
20. Bhandarkar U V, Swihart M T, Girshick S L and Kortshagen U R 2000 *J. Phys. D: Appl. Phys.* **33** 2731-2746
21. De Bleecker K, Bogaerts A, Goedheer W J and Gijbels R 2004 *IEEE Trans. Plasma Sci.* **32** 691-698
22. De Bleecker K, Bogaerts A, Gijbels R and Goedheer W 2004 *Phys. Rev. E* **69** 056409

23. Goree J 1994 *Plasma Sources Sci. Technol.* **3** 400-406
24. Trigger S A, Schram P P J M 1999 *J. Phys. D: Appl. Phys.* **32** 234-239
25. Choi S J and Kushner M J 1994 *IEEE Trans. Plasma Sci.* **22** 138-150
26. Barnes M S, Keller J H, Forster J C, O'Neill J A and Coultas D K 1994 *Phys. Rev. Lett.* **68** 313-316
27. Perrin J, Molinàs-Mata P and Belenguer Ph 1994 *J. Phys. D: Appl. Phys.* **27** 2499-2507
28. Akdim M R and Goedheer W 2003 *J. Appl. Phys.* **94** 104-109
29. De Bleecker K, Bogaerts A, Goedheer W and Gijbels R 2004 *Phys. Rev. E* **70** 056407
30. De Bleecker K, Bogaerts A and Goedheer W 2005 *Phys. Rev. E* **71** 066405
31. Liu X-M, Song Y-H, Xu X and Wang Y-N 2010 *Phys Rev E* **81** 016405
32. Kim K-S and Ikegawa M 1996 *Plasma Sources Sci. Technol.* **5** 311-322
33. Courteille C, Hollenstein Ch, Dorier J-L, Gay P, Schwarzenbach W, Howling A A, Bertran E, Viera G, Martins R and Mararico A 1996 *J. Appl. Phys.* **80** 2069-2078
34. Kortshagen U and Bhandarkar U 1999 *Phys. Rev. E* **60** 887-898
35. De Bleecker K, Bogaerts A and Goedheer W 2006 *New J. Phys.* **8** 178
36. Schweigert V A and Schweigert I V 1996 *J. Phys. D: Appl. Phys.* **29** 655-659
37. Lee K and Matsoukas T 1999 *J. Appl. Phys.* **85** 2085-2092
38. Lemons D S, Keinigs R K, Winske D and Jones M E 1996 *Appl. Phys. Lett.* **68** 613-615
39. Kim K-S and Kim D-J 2000 *J. Appl. Phys.* **87** 2691-2699
40. Kim K-S, Kim D-J, Yoon J-H, Park J Y, Watanabe Y and Shiratani M 2003 *J. Colloid Interface Sci.* **257** 195-207
41. Warthese S J and Girshick S L 2007 *Plasma Chem. Plasma Process.* **27** 292-310
42. Ravi L and Girschick S L 2010 *Phys. Rev. E* **79** 026408
43. Deschenaux Ch, Affolter A, Magni D, Hollenstein Ch and Fayet P 1999 *J. Phys. D: Appl. Phys.* **32** 1876-1886
44. Hong S, Berndt J and Winter J 2003 *J. Phys. D: Appl. Phys.* **12** 46-52
45. Stoykov S, Eggs C and Kortshagen U 2001 *J. Phys. D: Appl. Phys.* **34** 2160-2173
46. De Bleecker K, Bogaerts A and Goedheer W 2006 *Phys. Rev. E* **73** 026405
47. De Bleecker, Bogaerts A and Goedheer W 2006 *Appl. Phys. Lett.*. **88** 151501
48. Mao M, Benedikt J, Consoli A and Bogaerts A 2008 *J. Phys.D: Appl. Phys.* **41** 225201
49. Erdemir A, Bindal C, Fenske G R, Zuiker C, Krauss A R and Gruen D M 1996 *Diamond Relat. Mater.* **5** 923-931
50. Krauss A R *et al* 2001 *Diamond Relat. Mater.* **10** 1952-1961
51. Williams O A, Daenen M, D'Haen J, Haenen K, Maes J, Moshchalkov V V, Nesládek M and Gruen D M 2006 *Diamond Relat.Mater.* **15** 654-658
52. May P W, Harvey J N, Smith J A and Mankelevich Yu A 2006 *J. Appl. Phys.* **99** 104907
53. May P W 2000 *Philos. Trans. R. Soc. London A* **358** 473-495
54. Butler J E, Mankelevich Y A, Cheesman A, Ma J and Ashfold M N R 2009 *J. Phys.: Condens. Matter* **21** 364201
55. Cheesman A, Smith J A, Ashfold M N R, Langford N, Wright S and Duxbury G 2006 *J. Phys. Chem. A* **110** 2821-2828
56. Ma J, Cheesman A, Ashfold M N R, Hay K G, Wright S, Langford N, Duxbury G and Mankelevich Y A 2009 *J. Appl. Phys.* **106** 033305
57. Lombardi G, Hassouni K, Stancu G D, Mechold L, Röpcke J and Gicquel A 2005 *Plasma Sources Sci. Technol.* **14** 440-450
58. Lombardi G, Hassouni K, Bénédic F, Mohasseb F, Röpcke J and Gicquel A 2004 *J. Appl. Phys.* **96** 6739-6751
59. Teii K and Ikeda T 2007 *Appl. Phys. Lett.* **90** 111504
60. Rabeau J R, John P, Wilson J I B and Fan Y 2004 *J. Appl. Phys.* **96** 6724-6732

61. Gruen D M 1999 *Annu. Rev. Mater. Sci.* **29** 211-259
62. Mankelevich Y A, Rakhimov A T, Suetin N V 1998 *Diamond Relat. Mater.* **7** 1133-1137
63. May P W, Smith J A, Mankelevich Yu A 2006 *Diamond Relat. Mater.* **15** 345-352
64. May P W and Mankelevich Yu A 2006 *J. Appl. Phys.* **100** 024301
65. Mankelevich Yu A, Ashfold M N R and Orr-Ewing A J 2007 *J. Appl. Phys.* **102** 063310
66. Gordillo-Vázquez F J and Albella J M 2002 *Plasma Sources Sci. Technol.* **11** 498-512
67. Gordillo-Vázquez F J and Albella J M 2003 *J. Appl. Phys.* **94** 6085-6090
68. Gordillo-Vázquez F J and Albella J M 2004 *Plasma Sources Sci. Technol.* **13** 50-57
69. Hassouni K, Mohasseb F, Bénédic F, Lombardi G and Gicquel A 2006 *Pure Appl. Chem.* **78** 1127-1145
70. Bower C, Zhu W, Jin S and Zhou O 2000 *Appl. Phys. Lett.* **77** 830-832
71. Vizireanu S, Stoica S D, Luculescu C, Nistor L C, Mitu B and Dinescu G 2010 *Plasma Sources Sci. Technol.* **19** 034016
72. Denysenko I and Ostrikov K 2007 *Appl. Phys. Lett.* **90** 251501
73. Hash D, Bose D, Govindan T R and Meyyappan M 2003 *J. Appl. Phys.* **93** 6284–6290
74. Teo K B K *et al* 2004 *Nano Lett.* **4** 921-926
75. Hash D B, Bell M S, Teo K B K, Cruden B A, Milne W I and Meyyappan M 2005 *Nanotechnology* **16** 925–930
76. Bell M S, Teo K B K, Lacerda R G, Milne W I, Hash D B and Meyyappan M 2006 *Pure Appl. Chem.* **78** 1117-1125
77. Okita A, Suda Y, Ozeki A, Sugawara H, Sakai Y, Oda A and Nakamura J 2006 *J. Appl. Phys.* **99** 014302
78. Oda A, Suda Y and Okita A 2008 *Thin Solid Films* **516** 6570–6574
79. Delzeit L, McAninch I, Cruden B A, Hash D, Chen B, Han J and Meyyappan M 2002 *J. Appl. Phys.* **91** 6027-6033
80. Hash D and Meyyappan M 2003 *J. Appl. Phys.* **93** 750-752
81. Denysenko I B, Xu S, Long J D, Rutkevych P P, Azarenkov N A and Ostrikov K 2004 *J. Appl. Phys.* **95** 2713–2724
82. Yuji T and Sung Y M 2007 *IEEE Trans. Plasma Sci.* **35** 1027-1032
83. Ostrikov K, Yoon H J, Rider A E and Vladimirov S V 2007 *Plasma Process. Polym.* **4** 27–40
84. Mao M and Bogaerts A 2010 *J. Phys. D: Appl. Phys.* **43** 205201
85. Mao M and Bogaerts A 2010 *J. Phys. D: Appl. Phys.* **43** 315203
86. Ventzek P L G, Sommerer T J, Hoekstra R J and Kushner M J 1993 *Appl Phys Lett* **63** 605-607
87. Chhowalla M, Teo K B K, Ducati C, Rupesinghe N L, Amaratunga G A J, Ferrari A C, Roy D, Robertson J and Milne W I 2001 *J Appl Phys* **90** 5308-5317
88. Bell M S, Lacerda R G, Teo K B K, Rupesinghe N L, Amaratunga G A J, Milne W I and Chhowalla M 2004 *Appl Phys Lett* **85** 1137-1139
89. Matthews K, Cruden B A, Chen B, Meyyappan M and Delzeit L 2002 *J Nanosci Nanotechno* **2** 475-480
90. Cruden B A and Meyyappan M 2005 *J Appl Phys* **97** 084311
91. May P W, Allan N L, Ashfold M N R, Richley J C and Mankelevich Y A 2009 *J. Phys.: Condens. Matter* **21** 364203
92. Puretzky A A, Geohegan D B, Jesse S, Ivanov I N, and Eres G 2005 *Appl. Phys. A* **81** 223-240
93. Lee D H, Kim S O, and Lee W J 2010 **114** 3454-3458
94. Zhang Y and Smith K J 2005 *Journal of Catalysis* **231** 354-364

95. Naha S, Sen S, De A K, and Puri I K 2007 *Proceedings of the combustion institute* **31** 1821-1829
96. Naha S and Puri I K 2008 *J. Phys. D: Appl. Phys.* **41** 065304
97. Denysenko I and Ostrikov K 2007 *Appl. Phys. Lett.* **90** 251501
98. Denysenko I and Ostrikov K 2009 *J. Phys. D: Appl. Phys.* **42** 015208
99. Latorre N, Romeo E, Cazana F, Ubieto T, Royo C, Villacampa J I, and Monzon A 2010 *J. Phys. Chem. C* **114** 4773-4782
100. Grujicic M, Cao G and Gersten B 2002 *Applied Surface Science I* **191** 223-239
101. Lysaght A C and Chiu W K 2008 *Nanotechnology* **19** 165607
102. Lysaght A C and Chiu W K 2009 *Nanotechnology* **20** 115605
103. Hosseini M R, Jalili N and Bruce D A 2009 *AIChE Journal* **55** 3152-3167
104. Levchenko I and Ostrikov K 2008 *Appl. Phys. Lett.* **92** 063108
105. Levchenko I, Ostrikov K, Mariotti D, and Murphy A B 2008 *J. Appl. Phys.* **104** 073308
106. Levchenko I, Ostrikov K. Khachan J, and Vladimirov S V 2008 *Phys. Plasmas* **15** 103501
107. Tam E and Ostrikov K 2009 *Nanotechnology* **20** 375603
108. Agacino E and de la Mora P 2003 *Struct. Chem.* **14** 541-550
109. Kang J K and Musgrave C B 2000 *J. Chem. Phys.* **113** 7582-7587
110. Larsson K 1997 *Phys. Rev. B* **56** 15452-15458
111. Tamura H, Zhou H, Hirano Y, Takami S, Kubo M, Belosludov R V, Miyamoto A, Imamura A, Gamo M N and Ando T 2000 *Phys. Rev. B* **62** 16995-17003
112. Sternberg M, Zapol P and Curtiss L A, 2003 *Phys. Rev. B* **68** 205330
113. Gruen D M, Redfern P C, Horner D A, Zapol P and Curtiss L A 1999 *J. Phys. Chem. B* **103** 5459-5467
114. Cheesman, A, Harvey, J N and Ashfold, M N R 2008 *J. Phys. Chem. A* **112** 11436-11448
115. Tamura H and Gordon M S 2005 *Chem. Phys. Lett.* **406** 197-201
116. Gavillet J, Loiseau A, Journet C, Willaime F, Ducastelle F, Charlier J-C, 2001 *Phys. Rev. Lett.* **87** 275504
117. Gómez-Gualdrón D A, Balbuena P B, 2008 *Nanotechnology* **19** 485604
118. Amara H, Bichara C, Ducastelle F, 2008 *Phys. Rev. Lett.* **100** 056105
119. Charlier J-C, Amara H, Lambin Ph., 2007 *ACS Nano* **1** 202-207
120. Ohta Y, Okamoto Y, Page A J, Irle S, Morokuma K, 2009 *ACS Nano* **3** 3413-3420
121. Irle S, Ohta Y, Okamoto Y, Page A J, Wang Y, Morokuma K, 2009 *Nano Res.* **2** 755-767
122. Garrison B J, Kodali P B S and Srivastava D 1996 *Chem. Rev.* **96** 1327-1341
123. Brenner D W, 1990 *Phys. Rev. B* **42** 9458-9471
124. van Duin A C T, Dasgupta S, Lorant F, Goddard III W A, 2001 *J. Phys. Chem. A* **105** 9396-9409
125. Ostrikov K, Levchenko I, Xu S 2008 *Pure Appl. Chem*. **80** 1909-1918
126. Zhu W J, Pan Z Y, Ho Y K and Man Z Y 1999 Eur. Phys. J. D **5**, 83-88
127. Träskelin P, Salonen E, Nordlund K, Krasheninnikov A V, Keinonen J and Wu C H 2003 *J. Nucl. Mater*. **313-316** 52-55
128. Träskelin P, Saresoja O and Nordlund K 2008 *J. Nucl. Mater*. **375** 270-274
129. Eckert M, Neyts E and Bogaerts A 2008 *J. Phys. D: Appl. Phys.*. **41** 032006
130. Eckert M, Neyts E and Bogaerts A 2008 *Chem. Vapor Depos.* **14** 213-223
131. Garrison B J, Dawnkaski E J, Srivastava D and Brenner D W 1992 *Science* **255** 835-838
132. Metropolis N, Rosenbluth A W, Rosenbluth M N, Teller A H and Teller E 1953 *J. Chem. Phys.* **21** 1087-1092
133. Eckert M, Neyts E and Bogaerts A 2009 *CrystEngComm.* **11** 1597-1608

134. Eckert M, Neyts E and Bogaerts A 2010 *Crystal Growth & Design* **10** 3005-3021
135. Eckert M, Neyts E and Bogaerts A 2010 *Crystal Growth & Design* **10** 4123-4134
136. May P W and Mankelevich Y A 2008 *J. Phys. Chem. C* **112** 12432-12441
137. Netto A and Frenklach M 2005 *Diamond Relat. Mater.* **14** 1630-1646
138. Wagner R S, Ellis W C, 1964 *Appl. Phys. Lett.* **4** 89-90
139. Baker R T K, Barber M A, Harris P S, Feates F S and Waite R J, 1972 *J. Catal.* **26** 51-62
140. Helveg S, López-Cartes C, Sehested J, Hansen P L, Clausen B S, Rostrup-Nielsen J R, Abild-Pedersen F, Norskov J K, 2004 *Nature* **427** 426-429
141. Homma Y, Liu H, Takagi D, Kobayashi Y, 2009 *Nano Res.* **2** 793-799
142. Maiti A, Brabec C J, Roland C, Bernholc J, 1995 *Phys. Rev. B* **52** 14850-14858
143. Maiti A, Brabec C J, Bernholc J, 1997 *Phys. Rev. B* **55** R6097-R6100
144. Shibuta Y, Maruyama S, 2002 *Physica B* **323** 187-189
145. Shibuta Y, Maruyama S, 2003 *Chem. Phys. Lett.* **382** 381-386
146. Shibuta Y, Maruyama S, 2007 *Chem. Phys. Lett.* **437** 218-223
147. Martinez-Limia A, Zhao J, Balbuena P B, 2007 *J. Mol. Model.* **13** 595-600
148. Zhao J, Martinez-Limia A, Balbuena P B, 2005 *Nanotechnology* **16** S575-S581
149. Ribas M A, Ding F, Balbuena P B, Yakobson B I, 2009 *J. Chem. Phys.* **131** 224501
150. Ding F, Rosén A, Bolton K, 2005 *Carbon* **43** 2215-2217
151. Ding F, Rosén A, Bolton K, 2004 *J. Chem. Phys.* **121** 2775-2779
152. Ding F, Bolton K, Rosén A, 2006 *Comp. Mater. Sci.* **35** 243-246
153. Ding F, Rosén A, Bolton K, 2004 *Chem. Phys. Lett.* **393** 309-313
154. Voter A, Montalenti F, Germann T, 2002 *Ann. Rev. Mater. Res.* **32** 321-346
155. Neyts E, Shibuta Y, Bogaerts A, 2010 *Chem. Phys. Lett.* **488** 202-205
156. Dereli G, 1992 *Molec. Simul.* **8** 351-360
157. Timonova M, Groenewegen J, Thijsse B J, 2010 *Phys. Rev. B* **81** 144107
158. Neyts E C, Bogaerts A, 2009 *J. Phys. Chem. C* **113** 2771-2776
159. Neyts E, Shibuta Y, van Duin A C T, Bogaerts A, 2010 *ACS Nano*, in press (DOI: 10.1021/nn102095y)